American Journal of Mobile Systems, Applications and Services
Vol. 6, No. 2, 2020, pp. 23-28
http://www.aiscience.org/journal/ajmsas
ISSN: 2471-7282 (Print); ISSN: 2471-7290 (Online)

Voigt Function for the Investigation of the Optical Properties of the A-Plane Oriented ZnO: Case of the "A & B Excitons"

Alioune Aidara Diouf*, Bassirou Lo, Aboubaker Chedikh Béye

Faculty of Sciences and Techniques, Cheikh Anta Diop University of Dakar (UCAD), Dakar, Senegal

Abstract

The perpendicular polarization of the experimental reflectivity spectra at low temperature of the a-plane oriented ZnO grown on r-plane (011-2) sapphire substrates by plasma-assisted molecular beam epitaxy, shows two types of excitons A and B. The authors used a program based on the theory of the spatial resonance dispersion Hopfield model to fit the free excitons. But the main problem from the investigators were the use of the same Hopfiled model to fit the C free exciton obtained via a parallel polarization. That is why our goal in the present work, is to present our first results about the excitons A & B by using another method taking account the combination of two functions, Lorentzian and Gaussian. We've used as a computational method, the stepping by interval method. After calculations, we've fitted perfectly the excitons A and B using almost the same physical parameters than the theory of the spatial resonance dispersion Hopfield model. The numerical results show the positions of the A & B excitons energies exactly like the experimental results as displayed in the paper. In comparison, the numerical and experimental results are in good agreement. Otherwise, the same method has been used for beginning new calculations about the C-free exciton obtained from a parallel polarization, the results will be presented in our upcoming paper.

Keywords

Exciton A and B, Voigt Function, Reflectivity Spectrum, A-plane Oriented ZnO

Received: June 27, 2020 / Accepted: July 25, 2020 / Published online: August 26, 2020

1. Introduction

With its wide band gap (Eg = 3.37 eV) semiconductor, ZnO attracted investigators due to its potential applications [1-6]. ZnO has an important exciton band gap (60 meV) [7, 8], which makes for an intense near band-edge excitonic radiation at room and even higher temperatures.

Otherwise, the Photoluminescence spectra at low temperature of the a-plane oriented ZnO grown on r-plane (011-2) sapphire substrates by plasma-assisted molecular beam epitaxy, showed experimentally several types of excitons, in this paper we are going to focus on the A and B. The excitons transition from the conduction band to the valence bands or vice versa give information about two types of excitons A (also referred to as the heavy hole) and B (also referred to as the light hole). The selection rules for optical changes shows that A and B excitons have an important oscillator quality for $E \perp c$ (c represents the crystal axis). That is why in the photoluminescence spectrum one perceives their peaks in ZnO films with inaccurate energies and broad non-radiative damping constants. Subsequently, it is vital to analyze the excitonic releases of ZnO films in detail by using reflectivity for the affirmation of the peak position energies. Barely some studies have been done on a-plane ZnO [9, 10].

In this paper, one presents a spectroscopic investigation of a-plane-oriented ZnO developed by Molecular Beam Epitaxy

* Corresponding author
E-mail address: aliouneaidara.diouf@ucad.edu.sn (A. A. Diouf)

(MBE) on r-plane sapphire substrates. The optical properties of the a-plane ZnO films are examined by the reflectivity techniques. Also, we will use the Voigt function to model the experimental reflectivity of the excitons A and B. One will contrast our outcomes with those got in ref. [11, 12-14].

2. Experimental

A 1-μm-thick ZnO film was grown at temperature *Tg* ~500 °C. The growth was performed using solid-source Zn and a RF-activated plasma as the oxygen source. The growth rate was 0.2 μm/h, slightly lower than the optimal growth rate in a *c*-direction growth. Prior to growth, the *r*-plane (01–12) sapphire substrates were thermally cleaned and subsequently exposed to oxygen plasma during 5 to 10 min. The growth process was in situ monitored by reflection high energy electron diffraction (RHEED) and a streaky RHEED pattern was maintained throughout the growth, albeit with a slight modulation in the [1–100] azimuth. Ex situ surface morphology was investigated by means of atomic force microscopy (AFM). The structural properties were investigated by high resolution X-ray diffraction (HRXRD) experiments in high-resolution mode. Transmission electron microscopy (TEM) investigations were carried out in a JEOL 2010F field emission gun microscope. The results of these investigations are shown by the authors [15]. The optical properties of the structures were studied by using non-resonant photoluminescence excited with the 325 nm line from a He– Cd laser. The emitted light was dispersed using a 0.6 m focal length monochromator equipped with a 1200 lines/mm grating and detected by using a silicon photomultiplier tube (PMT) with conventional lock-in techniques. The chopping frequency was set at 220 Hz. The sample was mounted in an optical cryostat where the temperature could be varied from 8 to 300 K. Reflectivity measurements were obtained by exciting using a standard mercury bulb. Reflectivity studies were performed on the samples in the polarizations σ (respectively $E \perp c$ axes).

3. Formalism & Computational Method

To model the optical properties, we used the Voigt Function distribution defined by:

$$R(\omega, y) = \frac{\alpha y}{2\pi^2}\int_{-\infty}^{+\infty}\frac{e^{-\frac{\omega^2}{4\pi^2\Gamma^2}}}{y^2+(x-y)^5}d\omega + i\frac{\alpha}{2\pi^2}\int_{-\infty}^{+\infty}\frac{(x-\frac{\omega}{2\pi\Gamma})}{y^2+(x-\frac{\omega}{2\pi\Gamma})^2}e^{-\frac{\omega^2}{4\pi^2\Gamma^2}}d\omega \quad (1)$$

Where

$$x = \sqrt{\ln(2)}\frac{(\omega-\omega_0)}{2\pi\omega_D} \text{ and } y = \sqrt{\ln(2)}\frac{\omega_L}{\omega_D} \quad (2)$$

α_L: Lorentz half-width

α_D: Doppler half-width

$\alpha = \frac{4\pi N e_0^2}{m^*}$ With $e_0 = e/4\pi\varepsilon_0$ and $m^* = 0.59m_0$

R: Reflectivity

ω_0: Resonance frequency

α: Oscillator strength

N: Number of particles

e_0: Elementary charge electron

m*: Effective mass.

Γ: Spectral Widening

To plot the reflectivity, the numerical method of stepping by interval has been used, given by the function "bracketing" [16] in programming. The number of peak (n) observed in the experimental reflectivity is counted, and an interval (Δ_i) is built. For each interval, a Gaussian shape included in the Voigt function has been observed. However, with a program written according to the Voigt function, all the parameters above are considered as inputs for running the theoretical reflectivity program. With a test of convergence [16], we repeat this process for more accuracy with the experimental reflectivity [11], figure 1.

4. Results and Discussion

The experimental reflectivity of the ZnO films is displayed in the polarization E⊥c The emissions energies are found in the ranges 3.35-3.41 eV and 3.28-3.35 eV by experimental photoluminescence PL [11]. The reflectivity spectrum gives a clear resolution about the peak positions. In the E⊥c polarization at 8K, the reflectivity spectrum shows two free excitons owning to

the pre-eminence of the bound excitons at energy positions of 3.398 eV and 3.410 eV as depicted in figure 1. The two excitons as respectively denoted A and B as the heavy hole and the light hole. Otherwise, the energies of the different excitons were taken at the centers of the reflectivity peaks.

The Voigt function (1) has been used to model the reflectivity spectrum found experimentally as depicted in the figure 2. The fit parameters are (Γ) Spectral Widening, (ω_0) Lorentz half-width, (ω_D) Gaussian half-width, (ω_0) Resonance frequency, (α) Oscillator strength, (N) Number of particles, (e_0) Elementary charge electron, (m*) Effective masse. The effective mass is the same for both excitons and m_0 is the mass of a free electron. The excitons energies values measured at the peaks of the reflectivity, confirm the experimental reflectivity measurements. The value α of higher than 1 for the A free exciton is likely due to the fact that A is fitted together with B as displayed in figure 3. These results are in good agreement with the prediction of the selection rules of the optical transitions for the oscillator strength.

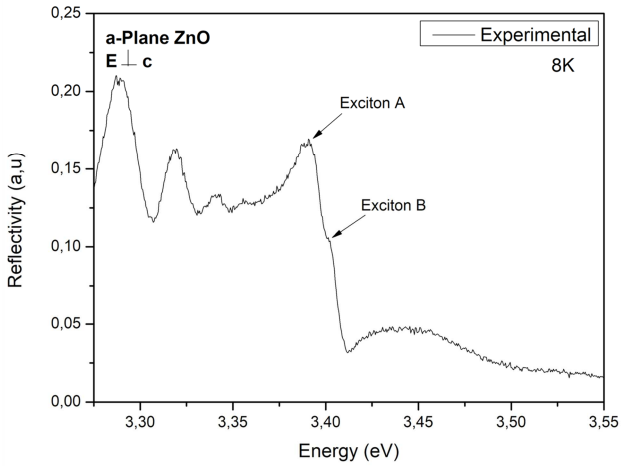

Figure 1. Experimental reflectivity of exciton A and B.

5. Conclusions

In summary, the temperature and polarization-dependent reflectivity of undoped *a*-plane ZnO have been investigated. The results indicate that our *a*-plane-oriented ZnO layer has a good optical property for more investigations. The A and B free exciton transitions have been identified. The energy positions of the free excitons as a function of temperature are presented. Otherwise, the A and B free excitons has been fitted by using the Voigt function and almost the same parameters than the Hopfield model.

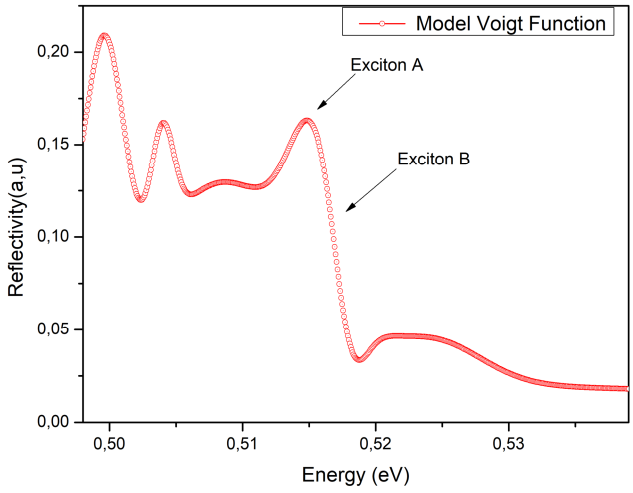

Figure 2. Theoretical reflectivity of exciton A and B.

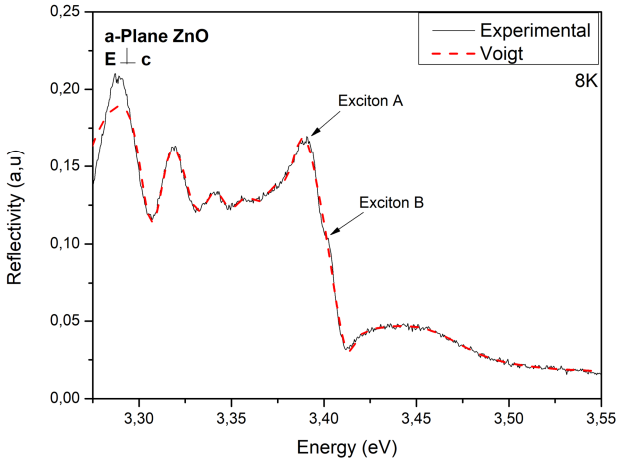

Figure 3. Experimental and Theoretical reflectivity of exciton A and B.

Acknowledgements

Dr. Bassirou Lo gratefully acknowledges about your help for the experimental results of the a-plane oriented ZnO. Pr. Beye thanks for your hospitality in your Laboratory at the University Cheikh Anta Diop of Dakar where i performed these results.

Appendix

Table 1. Values of A, B free excitons energies (eV), the spatial widening (Γ), the effective mass (m*) and the reflective curves obtained by using the Voigt function.

Free Exciton	Energy (eV)	Spectral widening (Γ) (m. s^{-1})	Effective mass (m*)	Oscillator Strength (α)
A	E=3.389eV	3.251E12 (Γ=2.14meV)	0.59m_0	1.71
B	E=3.401eV	3.996E14 (Γ=26.3meV)	0.59m_0	0.78

Table 2. Values of A and B free exciton Energy E (eV), Oscillator Strength (α), the spatial widening (Γ) and the effective mass (m*) of the exciton obtained by using the Hopfield model [11].

Free Exciton	Energy (E) (eV)	Oscillator Strength (α)	Spectral widening (Γ) (meV)	Effective mass (m*)
A	3.393	1.708	10.38	$0.59m_0$
B	3.403	0.77	11.479	$0.59m_0$

Table 3. Theoretical Data: From the Voigt Function.

Energy (eV)	Reflectivity (a. u)	Energy (eV)	Reflectivity (a. u)	Energy (eV)	Reflectivity (a. u)	Energy (eV)	Reflectivity (a. u)	Energy (eV)	Reflectivity (a. u)
0,49549	0,16688	0,50371	0,15746	0,5122	0,13159	0,52099	0,04624	0,53008	0,02632
0,49556	0,16384	0,50378	0,15897	0,51227	0,1322	0,52106	0,04631	0,53016	0,02609
0,49562	0,16084	0,50384	0,16019	0,51234	0,13286	0,52113	0,04637	0,53023	0,02587
0,49569	0,1579	0,50391	0,16108	0,51241	0,13355	0,5212	0,04642	0,5303	0,02565
0,49575	0,15503	0,50398	0,16165	0,51248	0,13429	0,52128	0,04646	0,53038	0,02543
0,49582	0,15225	0,50405	0,16187	0,51255	0,13507	0,52135	0,04648	0,53045	0,02523
0,49588	0,14955	0,50411	0,16176	0,51262	0,13588	0,52142	0,0465	0,53053	0,02502
0,49595	0,14696	0,50418	0,16133	0,51269	0,13673	0,52149	0,0465	0,5306	0,02482
0,49601	0,14448	0,50425	0,16057	0,51276	0,13762	0,52157	0,04651	0,53068	0,02462
0,49608	0,14212	0,50432	0,15953	0,51283	0,13855	0,52164	0,04651	0,53075	0,02443
0,49614	0,13989	0,50438	0,15822	0,5129	0,1395	0,52171	0,0465	0,53083	0,02424
0,49621	0,13781	0,50445	0,15666	0,51297	0,14049	0,52178	0,04649	0,5309	0,02406
0,49627	0,13587	0,50452	0,15491	0,51304	0,1415	0,52185	0,04648	0,53098	0,02388
0,49634	0,1341	0,50459	0,15298	0,51311	0,14254	0,52193	0,04647	0,53105	0,02371
0,49641	0,13249	0,50465	0,15093	0,51318	0,1436	0,522	0,04646	0,53113	0,02354
0,49647	0,13106	0,50472	0,14878	0,51325	0,14468	0,52207	0,04645	0,5312	0,02337
0,49654	0,12981	0,50479	0,14658	0,51332	0,14578	0,52214	0,04644	0,53128	0,02321
0,4966	0,12875	0,50486	0,14436	0,51339	0,14688	0,52222	0,04643	0,53135	0,02305
0,49667	0,12788	0,50492	0,14216	0,51346	0,148	0,52229	0,04642	0,53143	0,0229
0,49673	0,12722	0,50499	0,14	0,51353	0,14911	0,52236	0,04641	0,5315	0,02275
0,4968	0,12676	0,50506	0,13792	0,5136	0,15023	0,52243	0,0464	0,53158	0,0226
0,49686	0,12651	0,50513	0,13594	0,51367	0,15133	0,52251	0,04639	0,53165	0,02246
0,49693	0,12647	0,50519	0,13407	0,51374	0,15243	0,52258	0,04639	0,53173	0,02232
0,497	0,12665	0,50526	0,13234	0,51381	0,1535	0,52265	0,04638	0,5318	0,02219
0,49706	0,12704	0,50533	0,13075	0,51388	0,15456	0,52272	0,04637	0,53188	0,02206
0,49713	0,12764	0,5054	0,12932	0,51395	0,15558	0,5228	0,04636	0,53195	0,02193
0,49719	0,12846	0,50547	0,12804	0,51402	0,15657	0,52287	0,04634	0,53203	0,02181
0,49726	0,12949	0,50553	0,12692	0,51409	0,15751	0,52294	0,04633	0,5321	0,02169
0,49732	0,13073	0,5056	0,12595	0,51416	0,15841	0,52301	0,04632	0,53218	0,02157
0,49739	0,13217	0,50567	0,12514	0,51423	0,15925	0,52309	0,0463	0,53225	0,02146
0,49745	0,13381	0,50574	0,12446	0,5143	0,16002	0,52316	0,04628	0,53233	0,02135
0,49752	0,13564	0,50581	0,12392	0,51437	0,16073	0,52323	0,04626	0,5324	0,02125
0,49759	0,13766	0,50587	0,1235	0,51444	0,16135	0,5233	0,04624	0,53248	0,02115
0,49765	0,13984	0,50594	0,1232	0,51451	0,1619	0,52338	0,04621	0,53255	0,02105
0,49772	0,14219	0,50601	0,12299	0,51458	0,16235	0,52345	0,04619	0,53263	0,02095
0,49778	0,1447	0,50608	0,12288	0,51465	0,1627	0,52352	0,04615	0,5327	0,02086
0,49785	0,14734	0,50615	0,12285	0,51472	0,16294	0,5236	0,04611	0,53278	0,02077
0,49792	0,1501	0,50621	0,12289	0,51479	0,16307	0,52367	0,04607	0,53286	0,02068
0,49798	0,15298	0,50628	0,12298	0,51486	0,16307	0,52374	0,04603	0,53293	0,0206
0,49805	0,15595	0,50635	0,12313	0,51493	0,16294	0,52381	0,04598	0,53301	0,02052
0,49811	0,159	0,50642	0,12332	0,515	0,16268	0,52389	0,04592	0,53308	0,02044
0,49818	0,1621	0,50649	0,12354	0,51507	0,16228	0,52396	0,04586	0,53316	0,02036
0,49824	0,16526	0,50655	0,12378	0,51515	0,16172	0,52403	0,0458	0,53323	0,02029
0,49831	0,16843	0,50662	0,12405	0,51522	0,16101	0,52411	0,04573	0,53331	0,02022
0,49838	0,17161	0,50669	0,12432	0,51529	0,16013	0,52418	0,04565	0,53338	0,02015
0,49844	0,17478	0,50676	0,12461	0,51536	0,15909	0,52425	0,04557	0,53346	0,02008
0,49851	0,17791	0,50683	0,12491	0,51543	0,15787	0,52432	0,04548	0,53353	0,02001
0,49857	0,18098	0,50689	0,1252	0,5155	0,15648	0,5244	0,04538	0,53361	0,01995
0,49864	0,18399	0,50696	0,1255	0,51557	0,15491	0,52447	0,04528	0,53369	0,01989
0,49871	0,1869	0,50703	0,12579	0,51564	0,15315	0,52454	0,04518	0,53376	0,01983
0,49877	0,1897	0,5071	0,12608	0,51571	0,15122	0,52462	0,04506	0,53384	0,01978
0,49884	0,19237	0,50717	0,12636	0,51578	0,1491	0,52469	0,04495	0,53391	0,01972
0,4989	0,1949	0,50724	0,12663	0,51585	0,14679	0,52476	0,04482	0,53399	0,01967
0,49897	0,19726	0,5073	0,12689	0,51592	0,14431	0,52484	0,04469	0,53406	0,01962
0,49904	0,19944	0,50737	0,12714	0,51599	0,14165	0,52491	0,04455	0,53414	0,01957
0,4991	0,20142	0,50744	0,12738	0,51606	0,13881	0,52498	0,0444	0,53422	0,01952
0,49917	0,2032	0,50751	0,1276	0,51613	0,13581	0,52506	0,04425	0,53429	0,01947

Energy (eV)	Reflectivity (a. u)	Energy (eV)	Reflectivity (a. u)	Energy (eV)	Reflectivity (a. u)	Energy (eV)	Reflectivity (a. u)	Energy (eV)	Reflectivity (a. u)
0,49924	0,20476	0,50758	0,12782	0,5162	0,13264	0,52513	0,04409	0,53437	0,01943
0,4993	0,20609	0,50765	0,12802	0,51627	0,12933	0,5252	0,04393	0,53444	0,01939
0,49937	0,20718	0,50771	0,12821	0,51635	0,12587	0,52528	0,04376	0,53452	0,01934
0,49943	0,20802	0,50778	0,12839	0,51642	0,12228	0,52535	0,04358	0,5346	0,0193
0,4995	0,20861	0,50785	0,12855	0,51649	0,11858	0,52542	0,0434	0,53467	0,01926
0,49957	0,20894	0,50792	0,12871	0,51656	0,11477	0,5255	0,0432	0,53475	0,01922
0,49963	0,20901	0,50799	0,12884	0,51663	0,11088	0,52557	0,04301	0,53482	0,01919
0,4997	0,20882	0,50806	0,12897	0,5167	0,10691	0,52564	0,04281	0,5349	0,01915
0,49976	0,20837	0,50813	0,12908	0,51677	0,10289	0,52572	0,0426	0,53497	0,01912
0,49983	0,20766	0,50819	0,12918	0,51684	0,09883	0,52579	0,04238	0,53505	0,01908
0,4999	0,2067	0,50826	0,12927	0,51691	0,09475	0,52586	0,04216	0,53513	0,01905
0,49996	0,2055	0,50833	0,12934	0,51698	0,09068	0,52594	0,04193	0,5352	0,01902
0,50003	0,20406	0,5084	0,1294	0,51705	0,08663	0,52601	0,0417	0,53528	0,01899
0,5001	0,20239	0,50847	0,12944	0,51713	0,08263	0,52608	0,04147	0,53536	0,01896
0,50016	0,2005	0,50854	0,12948	0,5172	0,07868	0,52616	0,04122	0,53543	0,01893
0,50023	0,1984	0,50861	0,1295	0,51727	0,07482	0,52623	0,04098	0,53551	0,0189
0,5003	0,19611	0,50867	0,12951	0,51734	0,07106	0,5263	0,04072	0,53558	0,01887
0,50036	0,19364	0,50874	0,12951	0,51741	0,06742	0,52638	0,04047	0,53566	0,01884
0,50043	0,191	0,50881	0,1295	0,51748	0,06391	0,52645	0,0402	0,53574	0,01881
0,5005	0,18822	0,50888	0,12947	0,51755	0,06055	0,52652	0,03994	0,53581	0,01879
0,50056	0,1853	0,50895	0,12944	0,51762	0,05736	0,5266	0,03967	0,53589	0,01876
0,50063	0,18227	0,50902	0,12939	0,51769	0,05435	0,52667	0,0394	0,53596	0,01874
0,5007	0,17914	0,50909	0,12934	0,51777	0,05153	0,52674	0,03912	0,53604	0,01871
0,50076	0,17593	0,50916	0,12927	0,51784	0,0489	0,52682	0,03884	0,53612	0,01869
0,50083	0,17266	0,50922	0,1292	0,51791	0,04649	0,52689	0,03855	0,53619	0,01867
0,50089	0,16934	0,50929	0,12911	0,51798	0,04428	0,52697	0,03826	0,53627	0,01864
0,50096	0,166	0,50936	0,12902	0,51805	0,04229	0,52704	0,03797	0,53635	0,01862
0,50103	0,16265	0,50943	0,12892	0,51812	0,04052	0,52711	0,03768	0,53642	0,0186
0,50109	0,15931	0,5095	0,12882	0,51819	0,03896	0,52719	0,03739	0,5365	0,01858
0,50116	0,156	0,50957	0,12871	0,51826	0,03761	0,52726	0,03709	0,53658	0,01856
0,50123	0,15274	0,50964	0,12859	0,51834	0,03647	0,52733	0,03679	0,53665	0,01854
0,50129	0,14954	0,50971	0,12847	0,51841	0,03553	0,52741	0,03649	0,53673	0,01852
0,50136	0,14641	0,50978	0,12835	0,51848	0,03479	0,52748	0,03619	0,5368	0,0185
0,50143	0,14339	0,50985	0,12822	0,51855	0,03423	0,52756	0,03588	0,53688	0,01848
0,5015	0,14048	0,50991	0,12809	0,51862	0,03384	0,52763	0,03558	0,53696	0,01846
0,50156	0,13769	0,50998	0,12796	0,51869	0,03361	0,5277	0,03527	0,53703	0,01844
0,50163	0,13506	0,51005	0,12783	0,51876	0,03353	0,52778	0,03497	0,53711	0,01842
0,5017	0,13258	0,51012	0,12771	0,51884	0,03358	0,52785	0,03466	0,53719	0,0184
0,50176	0,13028	0,51019	0,12758	0,51891	0,03375	0,52793	0,03436	0,53726	0,01838
0,50183	0,12818	0,51026	0,12746	0,51898	0,03404	0,528	0,03405	0,53734	0,01836
0,5019	0,12628	0,51033	0,12735	0,51905	0,03441	0,52807	0,03375	0,53742	0,01835
0,50196	0,1246	0,5104	0,12724	0,51912	0,03486	0,52815	0,03344	0,53749	0,01833
0,50203	0,12316	0,51047	0,12714	0,51919	0,03538	0,52822	0,03314	0,53757	0,01831
0,5021	0,12196	0,51054	0,12705	0,51926	0,03595	0,5283	0,03284	0,53765	0,0183
0,50216	0,12102	0,51061	0,12697	0,51934	0,03656	0,52837	0,03253	0,53772	0,01828
0,50223	0,12035	0,51067	0,1269	0,51941	0,03719	0,52844	0,03223	0,5378	0,01826
0,5023	0,11996	0,51074	0,12684	0,51948	0,03785	0,52852	0,03193	0,53788	0,01824
0,50236	0,11985	0,51081	0,1268	0,51955	0,03851	0,52859	0,03164	0,53795	0,01823
0,50243	0,12002	0,51088	0,12678	0,51962	0,03917	0,52867	0,03134	0,53803	0,01821
0,5025	0,12048	0,51095	0,12678	0,51969	0,03981	0,52874	0,03105	0,53811	0,0182
0,50257	0,12123	0,51102	0,12679	0,51977	0,04045	0,52882	0,03076	0,53819	0,01818
0,50263	0,12226	0,51109	0,12683	0,51984	0,04106	0,52889	0,03047	0,53826	0,01816
0,5027	0,12356	0,51116	0,12689	0,51991	0,04164	0,52896	0,03019	0,53834	0,01815
0,50277	0,12512	0,51123	0,12698	0,51998	0,04219	0,52904	0,02991	0,53842	0,01813
0,50283	0,12692	0,5113	0,12709	0,52005	0,04271	0,52911	0,02963	0,53849	0,01812
0,5029	0,12894	0,51137	0,12723	0,52013	0,04319	0,52919	0,02935	0,53857	0,0181
0,50297	0,13115	0,51144	0,1274	0,5202	0,04363	0,52926	0,02908	0,53865	0,01809
0,50304	0,13352	0,51151	0,1276	0,52027	0,04404	0,52934	0,02881	0,53872	0,01807
0,5031	0,13601	0,51158	0,12783	0,52034	0,0444	0,52941	0,02854	0,5388	0,01806
0,50317	0,1386	0,51165	0,1281	0,52041	0,04473	0,52948	0,02828	0,53888	0,01804
0,50324	0,14124	0,51172	0,1284	0,52048	0,04503	0,52956	0,02802	0,53896	0,01803
0,5033	0,14388	0,51179	0,12874	0,52056	0,04529	0,52963	0,02776	0,53903	0,01801
0,50337	0,14649	0,51185	0,12912	0,52063	0,04552	0,52971	0,02751	0,53911	0,018
0,50344	0,14902	0,51192	0,12953	0,5207	0,04571	0,52978	0,02727	0,53919	0,01799
0,50351	0,15142	0,51199	0,12999	0,52077	0,04588	0,52986	0,02702	0,53926	0,01797
0,50357	0,15365	0,51206	0,13048	0,52084	0,04602	0,52993	0,02678	0,53934	0,01796

Energy (eV)	Reflectivity (a. u)	Energy (eV)	Reflectivity (a. u)	Energy (eV)	Reflectivity (a. u)	Energy (eV)	Reflectivity (a. u)	Energy (eV)	Reflectivity (a. u)
0,50364	0,15568	0,51213	0,13101	0,52092	0,04614	0,53001	0,02655		

References

[1] Oprea, Ovidiu, Andronescu Ecaterina, Ficao, Denisa, Ficai, Anton, N. Oktar, Faik, Yetmez, Mehmet, Bentham Science Publishers, Current Organic Chemistry, Volume 18, Number 2, 2014, pp. 192-203 (12).

[2] Ngom, I., Ndiaye, N., Fall, A., Bakayoko, M., Ngom, B., & Maaza, M. (2020). On the Use of Moringa Oleifera Leaves Extract for the Biosynthesis of NiO and ZnO Nanoparticles, MRS Advances, 5 (21-22), 1145-1155, doi: 10.1557/adv.2020.212.

[3] Alioune Aidara Diouf, Bassirou Lo, Balla Diop Ngom, Abib Fall, Aboubaker Chedikh Béye, International Journal of Advanced Materials Research, Vol. 4, No. 2, 2018, pp. 24-28.

[4] A. O. Kane, B. D. Ngom and O. Sakho, Influence of Adansonia digitata leaves dye extraction solvent nature on the structural and physical properties of biosynthesized ZnO nanoparticles, Materials Today: Proceedings, https://doi.org/10.1016/j.matpr.2020.04.048

[5] Alioune Aidara Diouf, Bassirou Lo, Oumar Sakho, Aboubaker Chedikh Beye, American Journal of Optics and Photonics. Vol. 5, No. 5, 2017, pp. 50-54.

[6] Mamadou. MBAYE, Ibrahima. NIANG, Bassirou. LO, Pape. M. WADE, Moustapha. BA, Mouhamed. B. GAYE, Alioune. A. DIOUF, B. DIOP. NGOM and Aboubaker. C. Beye. Journal of Applied Sciences and Research, 2016 April; 12 (4): pages 1-5.

[7] K. Hümmer, Phys. Status Solidi 56, 249 (1973).

[8] D. C. Look, Mater. Sci. Eng. B 80, 381 (2001).

[9] F. Liu, R. Zhang, Z. Hu, J. Sun, H. Huang, Z. Li, J. Zhao, P. Yin, L. Guo, X. Zhang, Y. Wang, IEEE Trans. Plasma Sci. 39 (2), 700 (2011).

[10] H. Lin, S. Zhou, J. Zhou, X. Liu, S. Gu, S. Zhu, Z. Xie, P. Han, R. Zhang, Thin Solid Films 516 (18), 6079 (2008).

[11] B. Lo, M. B. Gaye, A. Dioum, C. M. Mohrain, M. S. Tall, J. M. Chauveau, M. Doninelli Tesseire, S. Ndiaye, A. C. Beye, Appl. Phys. A (2014) 115: 257-261.

[12] T. Makino, Y. Segawa, M. Kawasaki, A. Ohtomo, Journal of Crystal Growth 287 (2006) 124–127.

[13] D. Tainoff, B. Masenelli, P. Mélinon, A. Belsky, G. Ledoux, D. Amans, C. Dujardin, N. Fedorov, P. Martin, Physical Review B 81, 115304 (2010).

[14] D. G. Thomas, J. Phys. Solids Pergamon Press 1960. Vol. 15. pp. 86-96.

[15] J. M. Chauveau, C. Morhain, B. Lo, B. Vinter, P. Vennéguès, M. Laügt, D. Buell, M. Tesseire-Doninelli, G. Neu, Appl. Phys. A 88, 65 (2007).

[16] Manfred Gilli, Méthodes Numériques, pp. 1-132 (2006).